Supplementary materials. Terahertz modulation of the Faraday effect by laser pulses.

A. Pump-probe time traces and corresponding frequency spectra

Pump induced polarization rotation dynamics was measured for different magnetic fields at a temperature of 1.7 K and a pump fluence of 10 mJ/cm^{-1} and is shown in Supplementary Fig. 1 (a). One can see that the oscillation dynamics is mostly dominated by one spectral component, the frequency of which varies from 0.1 THz to 1.1 THz with increasing the magnetic field from 100 G to 70 kG (Supplementary Fig. 1 (b)). We also observed a mode which at the field of 0.1 kG and 1.5 kG has a frequency of 1.3 THz. This second frequency is attributed to the pump induced coherence between the lowest quasi-doublet and the first excited state of the ground multiplet $^7F_6$ of the Tb^{3+} ion[1–5].

B. Pump induced paramagnetic resonance of Tb^{3+}

It has to be noted that by pumping $Tb_3Ga_5O_{12}$ with circularly polarized laser pulses the paramagnetic resonance precession of Tb^{3+} ions can be also excited. This mode corresponds to the pump induced coherence within the lowest quasi-doublet Tb^{3+} via impulsive stimulated Raman scattering. Supplementary figure 2(a) shows time traces of the pump induced probe polarization rotation signal in a magnetic field. The paramagnetic resonance signal decays exponentially within 70 ps and does not exhibit any abrupt quench at $\Delta\tau$=13 ps. The effective g-factor[6] was found to be g_{PMR}=7.5. One can compare the paramagnetic resonance mode and the oscillations due to the optical inhomogeneity discussed in the manuscript in Supplementary Fig. 2(b). We fitted the paramagnetic resonance mode with the following formula $\nu_{PMR} = \sqrt{\Delta^2 + (\mu_B \cdot g_{PMR} H/h)^2}$, where Δ is the crystal field splitting of the lowest quasi-doublet levels of a non-Kramers Tb^{3+} ion, μ_B is the Bohr magneton, h is the Planck constant.

C. Pump fluence dependence of the ultrafast polarization signal.

We measured the dependence of the frequency and amplitude of the ultrafast probe modulation on the pump fluence at a magnetic field of 30 kG and a temperature of 1.8 K. From Supplementary Fig. 3 one can see that the dependence of the amplitude on pump fluence is linear up to 50 mJ/cm^2, while the frequency remains constant in the measured fluence range.

D. Wavelength dependence of the oscillations associated with electronic transition in the Tb^{3+} ground multiplet

The oscillations arising from a homogeneous excitation have zero wave-vector and their coupling to visible light does not depend on its wavelength. Supplementary figure 4 shows the dependence of the frequency for the crystal field excitation and the paramagnetic resonance on the probe wavelength measured at B_0=20 kG and T=1.8 K. It is clear that the frequencies corresponding to electronic transitions within the ground multiplet of the Tb^{3+} ions were found to be independent of the probe wavelength.

E. Pump polarization dependence of ultrafast modulation signal

It is seen from Eq.(8) of the manuscript that the signal contains two components $\cos(\Omega\tau)$ and $\sin(\Omega\tau)$ which depend differently on the pump polarization angle Φ_{pu}. Supplementary figure 5 (a) shows the probe modulation for different Φ_{pu} at a magnetic field of 35 kG and a temperature of 1.7 K. One sees that the amplitude of the modulation is unchanged while the phase changes with changing the pump polarization. To check whether the observed behavior is consistent with our model, we performed a fit of the time traces in Supplementary Fig. 5 (a) as suggested by Eq.(8). One can see that this form describes perfectly the experimental data shown in Supplementary Fig. 5 (b). Indeed, the experimental signal is proportional to a $\sin(\Phi_{pu})\cos(\Omega\tau) + \cos(\Phi_{pu})\sin(\Omega\tau)$.

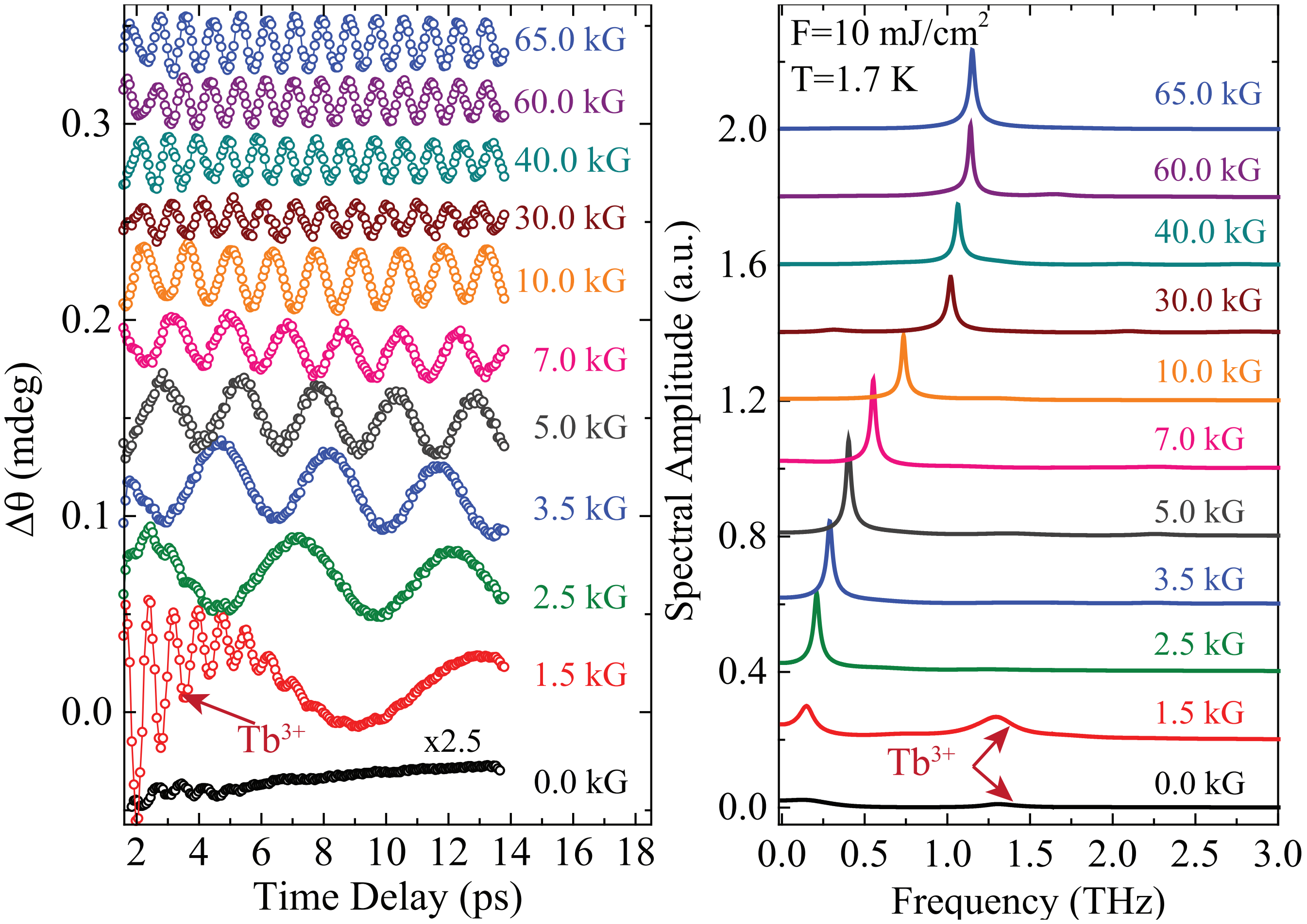

FIG. 1. (a) Temporal evolution of the pump induced probe polarization Faraday rotation for the range of magnetic fields of 0.1-70 kG at temperature 1.7 K. Pump was linearly polarized and had a fluence of F=10 mJ/cm^2. (b) Corresponding FFT spectra of measured pump-probe signal of the Faraday rotation. One can see the emergence of the frequency associated with the electronic transition in the Tb^{3+} ground multiplet in the small magnetic field with frequency of 1.33 THz.

One sees from Eq.(8) that the signal also has odd and even part with respect to the applied magnetic field, which was experimentally confirmed (see Supplementary material F).

F. Effect of the magnetic field polarity on the modulation signal

One sees from Eq.(8) that the signal should have odd and even parts with respect to the applied magnetic field. Indeed, we found that the modulation signal contains both odd and even components with respect to the external magnetic field, which is seen in Fig.6.

G. Comparison the modulation signal of transmitted and reflected probe

The laser induced transmissivity or reflectivity signals exhibit only a temporal overlap between the two laser pulses (Supplementary Fig. 7 (a,c)). The observed overlap duration of 1.5 ps exceeds that of the convolution of the pump and probe pulses because of their co-propagation with slightly different group velocities, that was confirmed by our calculations (see the inset in Supplementary Fig. 7 (a) and explanation in the Method sections). It is seen from Supplementary Fig. 7 (b and d) that the Faraday rotation signal shows oscillations which persist only in a limited time window: at a time delay of $\Delta\tau \approx 13$ ps the signal is abruptly quenched. The fast Fourier transform (FFT) spectra in Supplementary

Fig. 7 (e and f,g) of the signals in Supplementary Fig. 7 (b,d) respectively shows that the dominating oscillation frequency observed in transmission probe coincide with both frequencies measured the positive and negative delay for the reflected probe. The appearance of the oscillations in the negative delay discriminates them from any mode of the crystal, since otherwise it would contradict causality. Indeed, one sees from the spectra in Supplementary Fig. 7 (e,g) that in the positive delay probe does measure induced by the pump the electronic transitions in the Tb^{3+} ground multiplet (1.36 and 2.25 THz) and phonon modes (5.1 and 5.4 THz) of $Tb_3Ga_5O_{12}$[1,5]. Note that the oscillations in the negative delay are linked with the presence of the pump in the medium as the probe measures only pump induced signal. Thus, the observed oscillations in the Faraday rotation signal of the transmitted and reflected probe can be the sought magneto-optical modulation. In this case, the abrupt quench is due to the finite propagation time inside the crystal.

We can distinguish two situations which depend on the time delay between the two pulses. In the first case, the probe pulse propagates later than the pump pulse, with the time delay between the two pulses $\tau > 0$. Then the probe propagates through the reflected part of the pump pulse until the reflected pump reaches the front surface of the crystal. In the second case, the probe pulse propagates earlier than the pump pulse $\tau < 0$ and, thus, being reflected from the rear surface of the crystal counter propagates through the full pump. As a result, the polarization modulation of both the reflected and transmitted probe is achieved for $\tau > 0$, while the reflected probe is also modulated in $\tau < 0$. In the first case the modulation appears only after a temporal overlap between the pump and probe, while in the second it appears before and after the temporal overlap. In the both cases the probe polarization is modulated by the optical Kerr nonlinearity of the pump. The optical Kerr nonlinearity acts as linear dichroic or birefringent plate on the propagating through it probe. As a result probe acquires an additional time-dependent polarization rotation, that is the probe polarization modulation. One sees that the probe in the positive delay propagates through the weak reflected pump while in the negative delay it propagates through the full pump, which is confirmed by the experimental observation in Supplementary Fig. 7(d). The ratio $\approx$10 between the amplitudes of the signals in the both delays reasonably corresponds to a reflection coefficient of $\approx$10%.

H. Group refractive index as a function of wavelength.

To calculate the group refractive index of the $Tb_3Ga_5O_{12}$ we first calculate the normal refractive index of the material by the following formula:

$$n(\lambda) = \left(A + \frac{B}{\lambda^2 - C} - D\lambda^2 \right), \quad (1)$$

where A=3.73895, B=0.0516156 µm^2, C=-0.00115321 µm^2, D=0.00590524 µm^{-2}. The parameters are taken from Ref. 7. To calculate group refractive index the following formula is used:

$$n_g(\lambda) = \left(n(\lambda)^{-1} + \frac{\lambda}{n^2(\lambda)} \cdot \frac{\partial n(\lambda)}{\partial \lambda} \right)^{-1} \quad (2)$$

Supplementary Fig.8 shows both the refractive and group refractive indices of $Tb_3Ga_5O_{12}$in visible and near infrared range.

I. FFT spectrum of $Tb_3Ga_5O_{12}$ at 65 kG.

We measured FFT spectrum seen in Supplementary Fig. 9 of the probe Faraday rotation signal at a magnetic field of 65 kG oriented in the plane of the sample. Temperature was 1.7 K. Probe wavelength is 0.4 µm. We found a frequencies associated with transitions between levels of the ground multiplet of the Tb^{3+} ion. Also one can see that the mode with frequencies up to 7.27 THz were observed[1,5].

[1] Gavignet-Tillard, A., Hammann, J. & De Seze, L. Crystal-field splitting of the fundamental multiplet of Tb3+ in terbium aluminum garnet. J. Phys. Chem. Solids **34**, 241–248 (1973). URL http://linkinghub.elsevier.com/retrieve/pii/0022369773900838.

[2] Bayerer, R., Heber, J. & Mateika, D. Crystal-field analysis of Tb3+ doped yttrium aluminium garnet using site-selective polarized spectroscopy. Zeitschrift fur Phys. B Condens. Matter **64**, 201–210 (1986).

[3] Valiev, U. V. et al. Zeeman effect and stark splitting of the electronic states of the rare-earth ion in the paramagnetic terbium garnets Tb3Ga5O12 and Tb3Al5O12. Phys. Solid State **49**, 91–98 (2007). URL http://link.springer.com/10.1134/S1063783407010167.

[4] Valiev, U. V. et al. Specific features of magneto-optical spectra of Tb3Ga5O12. Opt. Spectrosc. **102**, 910–917 (2007). URL http://link.springer.com/10.1134/S0030400X07060185.

[5]Gruber, J. B. et al. Analyses of the optical and magneto-optical spectra of Tb[sub 3]Ga[sub 5]O[sub 12]. J. Appl. Phys. **101**, 023108 (2007). URL http://link.aip.org/link/JAPIAU/v101/i2/p023108/s1\&Agg=doi.

[6]Löw, U. et al. Magnetization, magnetic susceptibility and ESR in Tb3Ga5O12. Eur. Phys. J. B **86**, 87 (2013). URL http://link.springer.com/10.1140/epjb/e2012-30993-0.

[7]Villora, E. G. et al. Faraday rotator properties of {Tb3}[Sc1.95Lu0.05](Al3)O12, a highly transparent terbium-garnet for visible-infrared optical isolators. Appl. Phys. Lett. **99**, 011111 (2011).

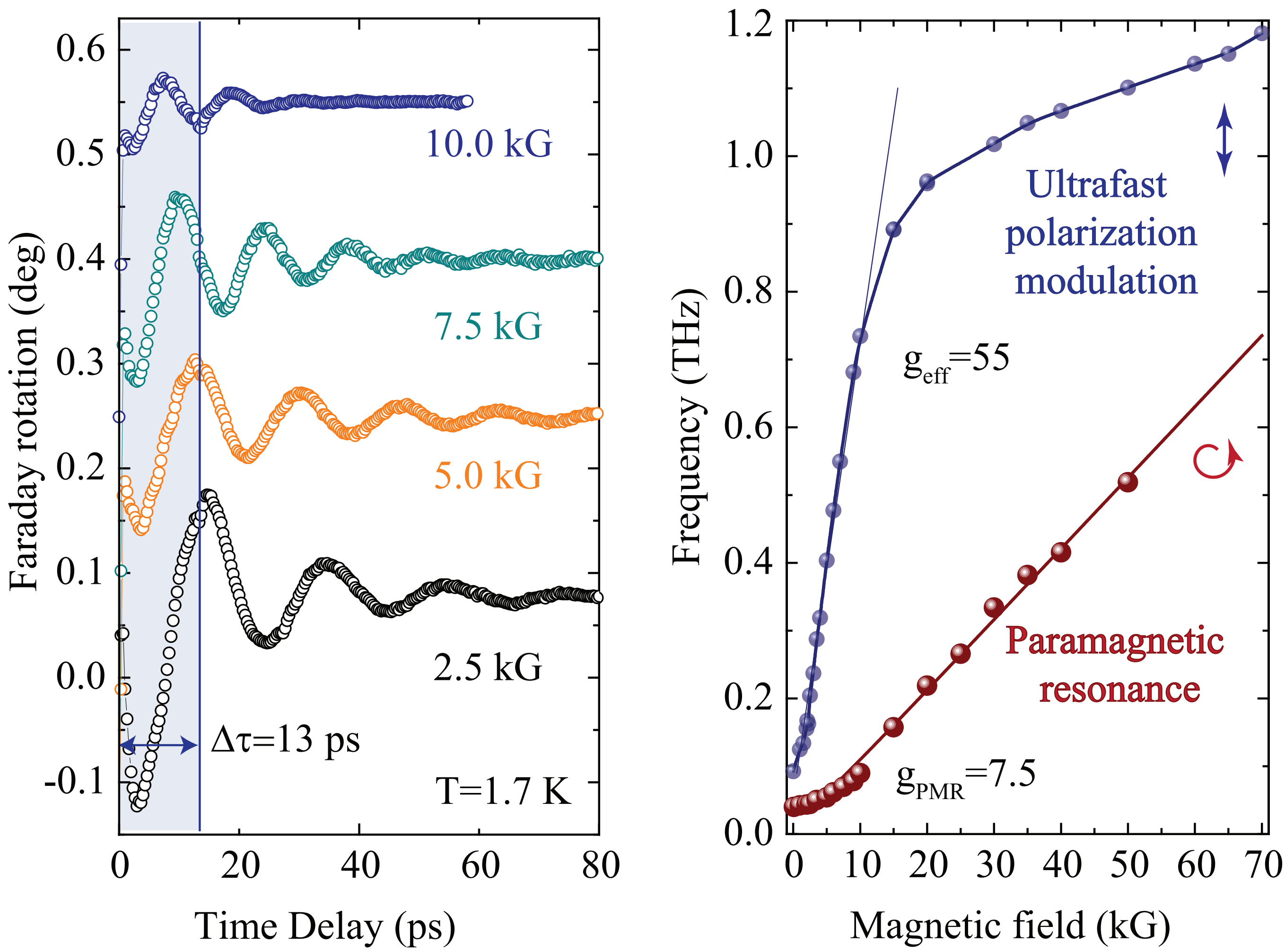

FIG. 2. **Paramagnetic resonance Tb^{3+}**(a) Temporal evolution of the pump induced probe polarization Faraday rotation for a range of magnetic fields of 2.5-10 kG at 1.7 K. Pump was circularly polarized and had a fluence of F=10 mJ/cm^2. The shaded area marked with the double arrow is the time window $\Delta\tau$=13 ps where the ultrafast polarization mode exists. (b) The frequency of the paramagnetic resonance mode and the ultrafast polarization modulation as function of applied magnetic field at 1.7 K and a probe wavelength of 0.4 μm.

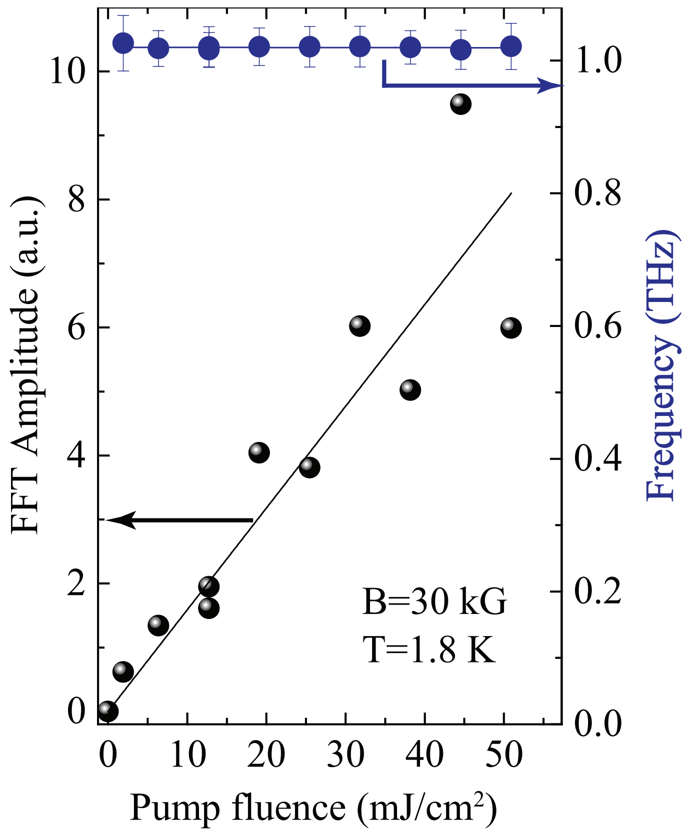

FIG. 3. **Fluence dependence of the modulation signal.** Pump fluence dependence of the amplitude and frequency of the ultrafast modulation at a magnetic field of 30 kG and temperature of 1.8 K. Lines are the linear fits.

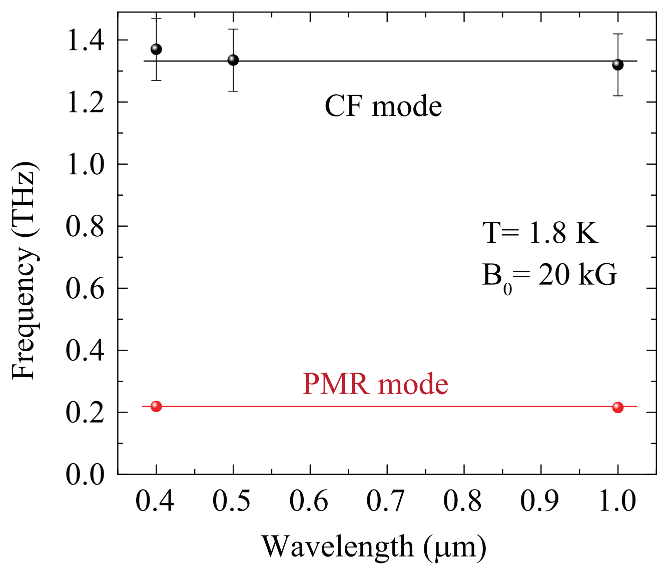

FIG. 4. Wavelength dependence of the oscillations associated with electronic transition within the lowest quasi doublet (paramagnetic resonance) and between the quasi doublet and the first excited levels of the ground multiplet of the Tb^{+3} ion. The former resonance is excited by the circularly polarized laser pulses, the former one is excited by the linearly and circularly polarized pulses. In all measurements magnetic field is 20 kG and temperature is 1.8 K.

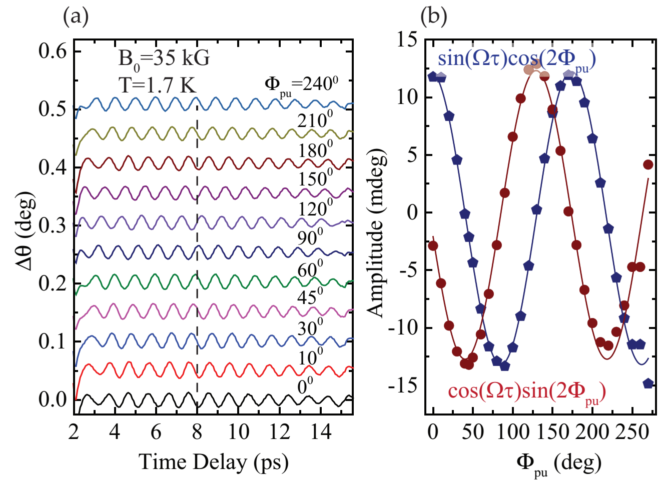

FIG. 5. **Dependence of the modulation on the pump polarization azimuth.** (a) Time traces of the probe Faraday rotation for different azimuth of pump polarization at a probe wavelength of λ_{probe} =0.4 µm, B_0=35 kG and T=1.7 K. (b) Amplitudes of the sine $\sin(\Omega\tau)$ and cosine $\cos(\Omega\tau)$ like contributions of the signal shown in panel (a) as the function of pump polarization azimuth Φ_{pu}

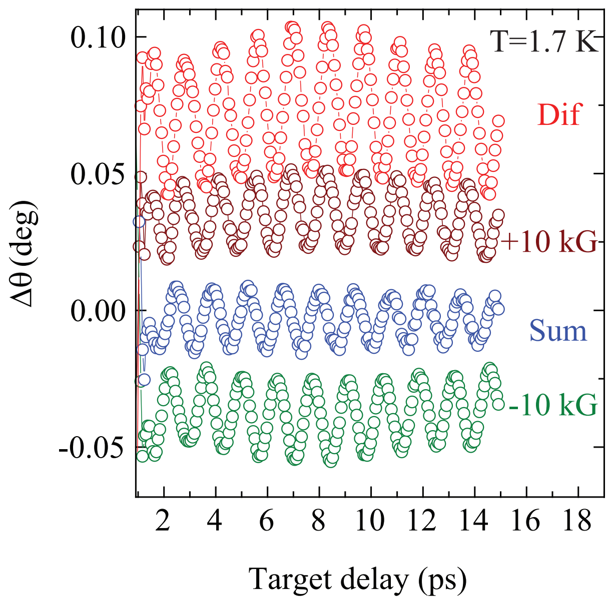

FIG. 6. **Dependence of the modulation on the magnetic field polarity.** Effect of the magnetic field polarity on the modulation signal at a temperature of 1.7 K and magnetic field 10 kG. Dif and Sum are the signal obtained as $\Delta\theta(B_0+) - \Delta\theta(B_0-)$ and $\Delta\theta(B_0+) + \Delta\theta(B_0-)$, respectively.

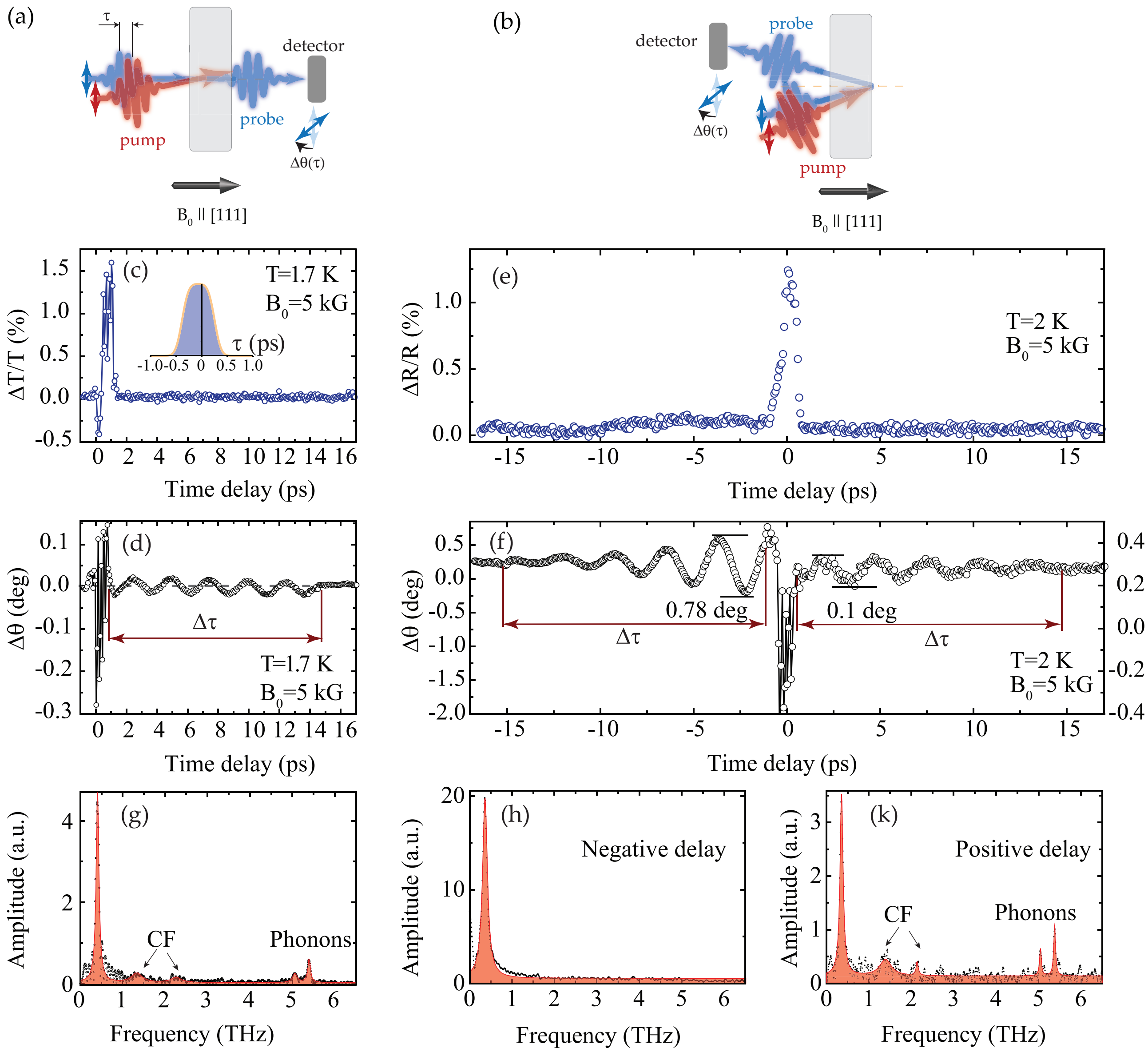

FIG. 7. **Experimental observation of the ultrafast polarization modulation.** (a,b) Typical temporal response of the pump induced transmissivity changes and polarization rotation of the transmitted probe, respectively, at 5 kG and 1.7 K. Arrow shows the limited time window of the observed oscillations. (c,d) Typical temporal response of the pump induced reflectivity changes and polarization rotation of the reflected probe, respectively, at 5 kG and 2 K. Vicinity of the 0 ps corresponds to the temporal overlap. (e) FFT spectrum of the signal shown in panel (b) in the positive delay. (f,g) FFT spectra of signal shown in panel (d) in the negative and positive delay, respectively.

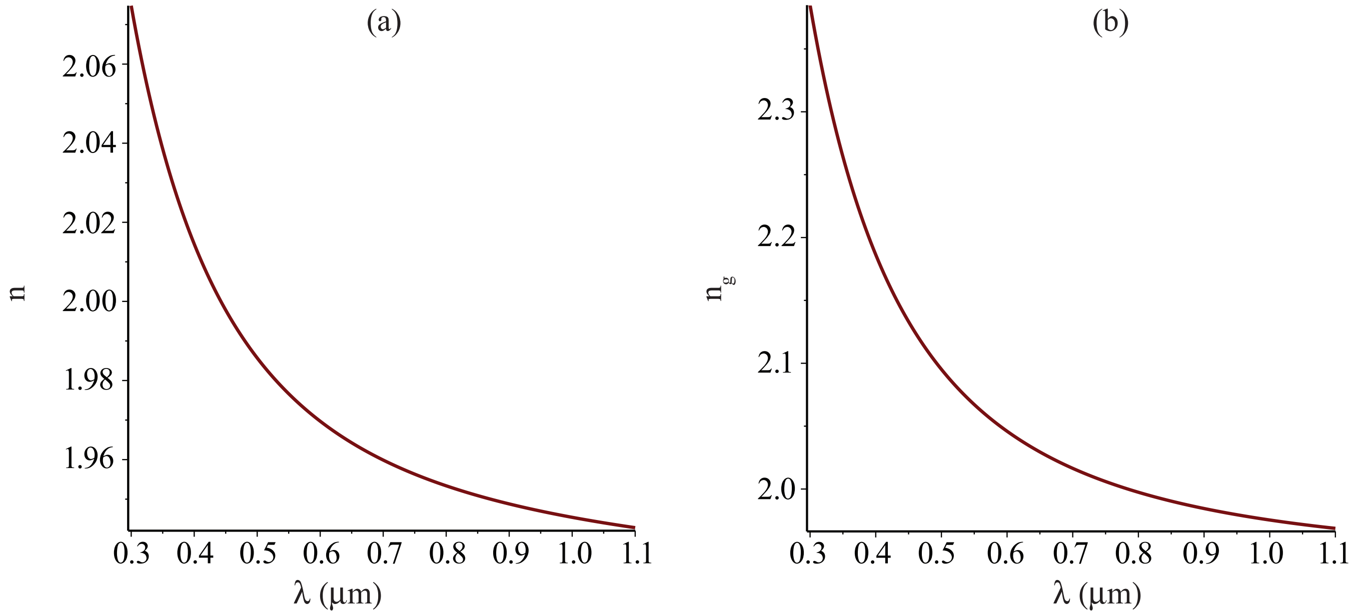

FIG. 8. (a) Refractive index of $Tb_3Ga_5O_{12}$. (b) Group refractive index of $Tb_3Ga_5O_{12}$

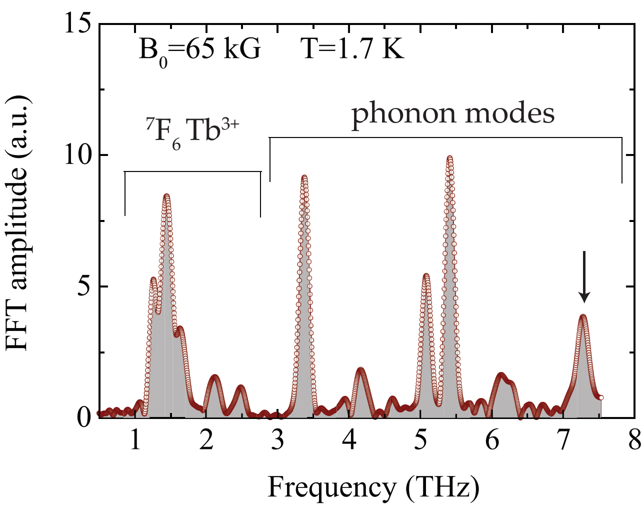

FIG. 9. FFT spectrum of the probe Faraday rotation signal measured at a magnetic field of 65 kG oriented in the plane of the sample. Temperature was 1.7 K. Probe wavelength is 0.4 μm.